Supporting Information

Horan et al. 10.1073/pnas.1005431108

SI Text S1: Model Specification and Parameterization

Ecological Model. Consider a closed lake ecosystem and denote crayfish and bass biomass at time τ as X and Y, respectively. Following Drury and Lodge (1), the IGP model is specified as

$$\frac{dX}{d\tau} = r_x X\left(1 - \frac{X}{K_x} - \frac{\alpha_{yx}Y}{K_x}\right) - \frac{\delta_{yx}YX^2}{k^2 + X^2} + e_x gXY - h_X, \quad [S1]$$

$$\frac{dY}{d\tau} = r_y Y\left(1 - \frac{\alpha_{xy}X}{K_y} - \frac{Y}{K_y}\right) + \frac{e_y \delta_{yx}YX^2}{k^2 + X^2} - gXY - h_Y. \quad [S2]$$

In Eqs. S1 and S2, r_x and r_y are, respectively, crayfish and bass intrinsic rates of increase, α_{ij} is the interspecific competitive effect of species i on species j's population growth ($i, j = x, y; i \neq j$), K_x and K_y are, respectively, crayfish and bass carrying capacities, δ_{yx} is the maximum bass attack rate on crayfish, and k is the crayfish density at which bass attack rates are half-maximal. The second term in Eqs. S1 and S2 is a type III functional response, arising because cobble provides crayfish refuge from bass predation (2, 3). The parameters e_x and e_y are conversion efficiencies, g is the maximum attack rate of crayfish on bass eggs, and h_X and h_Y are harvests by humans.

Eqs. **1** and **2** are based on a nondimensionalized (rescaled) version of the model, as presented in Drury and Lodge (1). The nondimensionalized model is

$$\frac{dx}{dt} = \dot{x} = x(1 - x - \alpha y) - \frac{\delta y x^2}{\kappa^2 + x^2} - h_x = F(x,y) - h_x, \quad [S3]$$

$$\frac{dy}{dt} = \dot{y} = ry(1 - \beta x - y) + \varepsilon\frac{\delta y x^2}{\kappa^2 + x^2} - h_y = G(x,y) - h_y \quad [S4]$$

where $x = X/K_x$, $y = Y/K_y$, $h_x = h_X/K_x$, and $h_y = h_Y/K_y$ are the states and controls expressed in densities. The time index has been scaled as $t = r_x\,\tau$. Other parameters have been scaled as $\alpha = \alpha_{yx}K_y/K_x - e_x g/r_x$, $\beta = [\alpha_{xy} + g/r_y]K_x/K_y$, $\delta = [\delta_{yx}/r_x]K_y/K_x$, $\kappa = k/K_x$, $\varepsilon = e_y K_x/K_y$, and $r = r_y/r_x$. Model parameters are from Drury and Lodge (1) and, along with the economic parameters, are presented in Table S1.

Economic Model. Angler net benefits of harvesting at time τ are specified as

$$B(h_Y, Y) = (P_y - w_y/Y)h_y, \quad [S5]$$

where P_y is the fixed marginal value of harvested bass, w_y/Y is the unit cost of bass harvests, and w_y is a cost parameter. The cost relation is common (4) and assumes unit costs decline in the bass stock, as bass are easier to catch when more abundant. Crayfish removal costs at time τ are

$$C(h_X, X) = w_x h_X/X. \quad [S6]$$

Defining ρ_τ as the discount rate, the economic social welfare from bass and crayfish harvests is represented by the present value

$$\mathrm{SW} = \int_0^\infty \left[(P_y - w_y/Y)h_Y - w_x h_X/X\right]e^{-\rho_\tau \tau}d\tau. \quad [S7]$$

The economic relations in Eqs. S5–S7 depend on the nonscaled state and control variables. To work with the scaled variables, we rescale the model without altering B, C, or SW. Setting $p = P_y K_y$ (and leaving w_y unscaled), angler net benefits at time t are

$$B(h_y, y) = (p - w_y/y)h_y. \quad [S8]$$

$B(h_y, y)$ is unaffected by the rescaling, nor are crayfish removal costs or the parameter w_x affected. The rescaled discount rate is $\rho = \rho_\tau/r_x$ (to account for the new timescale), so SW is

$$\mathrm{SW} = \int_0^\infty \left[(p - w_y/y)h_y - w_x h_x/x\right]e^{-\rho t}dt. \quad [S9]$$

SW is unaffected by the rescaling. We have chosen realistic parameters (Table S1) for illustrative purposes. Accordingly, the bioeconomic results should be viewed as a numerical example designed to illustrate the concept of bioeconomically derived thresholds.

SI Text S2: The Bioeconomic Model and Solution

Bioeconomic Problem. The bioeconomic problem is

$$\begin{aligned} \underset{h_y, h_x \mathit{iff} \in \Omega}{\mathrm{Max}} \quad & \mathrm{SW} = \int_0^\infty \left[(p - w_y/y)h_y - w_x h_x/x\right]e^{-\rho t}dt \\ s.t. \quad & (\mathrm{Eq.\ S1}),\ (\mathrm{Eq.\ S2}),\ x(0) = x_0,\ y(0) = y_0 \\ & h_x = 0 \quad \mathit{iff} \quad h_x \notin \Omega,\ h_y = h_y^{\mathrm{OA}}(y,x) \quad \mathit{iff} \quad h_y \notin \Omega. \end{aligned} \quad [S10]$$

Problem Eq. S10 is a linear control problem with potential institutional constraints on one or more of the controls such that h_x or h_y may not be in Ω. Here, we assume $h_i \in \Omega$ for $i = x$ or $i = y$ or both. The case of $\Omega = \{\}$ is scenario I in the main text.

The current value Hamiltonian (henceforth, referred to as the Hamiltonian) for problem Eq. S10, in the institutionally unconstrained case, is

$$H = (p - w_y/y)h_y - w_x h_x/x + \lambda_y[G(x,y) - h_y] + \lambda_x[F(x,y) - h_x], \quad [S11]$$

where λ_i is the costate variable associated with state variable $i = x, y$. The Hamiltonian is modified in the constrained cases by substituting either $h_x = 0$ or $h_y = h_y^{\mathrm{OA}}(y)$ directly into Eq. S11. Regardless of these constraints, the following adjoint condition holds along an optimal path:

$$\dot{\lambda}_i = \rho\lambda_i - \partial H/\partial i, i = x, y. \quad [S12]$$

The following subsections examine the permutations of institutional constraints on the controls.

Scenario II: Managing Crayfish but Not Bass. Suppose the agency can choose crayfish harvests but is unable to regulate bass harvests [i.e., $\Omega = \{h_x\}$, and $h_y = h_y^{\mathrm{OA}}(y)$]. Under open access, anglers adjust harvest levels until economic rents dissipate; i.e., $p - w_y/y = 0$. When $y > w_y/p$ (i.e., positive rents), open access harvests, $h_y^{\mathrm{OA}}(y)$, are large enough to dissipate rents and move the system to $y = w_y/p$. When $y < w_y/p$ (i.e., negative rents), then $h_y^{\mathrm{OA}}(y) = 0$ and the stock recovers. The outcome $y = w_y/p$ is an equilibrium for y and implies the equilibrium condition $h_y^{\mathrm{OA}} = G(x,y) = G(x, w_y/p)$.

For simplicity, suppose anglers immediately transition the system to dissipate rents (i.e., $y = w_y/p$; without instantaneous adjustment, the long-run result is the same, but the approach path may involve dampened oscillations involving intervals of

positive and negative rents) (4). Given this equilibrium outcome in the bass sector,

$$\mathrm{SW} = \int_0^\infty [-w_x h_x / x] e^{-\rho t} dt. \qquad \textbf{[S13]}$$

Eq. S13 implies there is no incentive to harvest crayfish ($h_x = 0$). Doing so only generates costs with no offsetting benefits in the bass sector (due to dissipated rents in that sector).

The phase plane is presented in Fig. 4 (main text). The $dx/dt = 0$ isocline and associated phase arrows are the same as in the decoupled model (Fig. 3, main text). The $dy/dt = 0$ isocline is horizontal, given by the economic equilibrium condition $y = w_y/p$. The phase arrows are consistent with moving to this equilibrium value for y. Together, the isoclines and phase arrows indicate point A is a globally stable equilibrium.

Scenario III: Managing Bass but Not Crayfish. Suppose the agency can choose bass harvests, but has no authority or budget to manage crayfish harvests; i.e., $h_x = 0$. To conserve on space in later sections, we begin by deriving the optimality conditions for h_y for the more general case in which h_x is not constrained and then impose the condition $h_x = 0$. The marginal effect of bass harvests on the Hamiltonian Eq. S11 is

$$\partial H/\partial h_y = \sigma_y = p - w_y / y - \lambda_y, \qquad \textbf{[S14]}$$

where σ_y is defined as the linear coefficient of h_y in the Hamiltonian and is referred to as the switching function for h_y (4). If $\sigma_y < 0$, no bass harvests should take place ($h_y = 0$) as the marginal value of bass harvests is negative. If $\sigma_y > 0$, then more bass harvests always add value and so h_y should be set as large as possible. A singular path for h_y is followed when $\sigma_y = 0$. The optimal level of h_y follows a feedback rule, denoted $h_y(x, y)$, defined by

$$h_y(x,y) = \begin{cases} h_y^{\max} & \textit{iff} \quad \sigma_y > 0 \\ h_y^*(x,y) & \textit{iff} \quad \sigma_y = 0 \\ 0 & \textit{iff} \quad \sigma_y < 0, \end{cases} \qquad \textbf{[S15]}$$

where the superscript * denotes the state variables are evaluated along a singular arc.

Consider the singular solution, in which case σ_y vanishes:

$$\lambda_y = p - w_y/y. \qquad \textbf{[S16]}$$

Taking the time derivative of Eq. S16 yields

$$\dot{\lambda}_y = \frac{w_y}{y^2}\,\dot{y} = \frac{w_y}{y^2}[G(x,y) - h_y]. \qquad \textbf{[S17]}$$

Substituting Eqs. S16 and S17 into the adjoint condition Eq. S12 for bass yields

$$\frac{w_y}{y^2}[G(x,y) - h_y] = \rho\left[p - \frac{w_y}{y}\right] - \frac{w_y h_y}{y^2} - \left[p - \frac{w_y}{y}\right]\frac{\partial G(x,y)}{\partial y} - \lambda_x \frac{\partial F(x,y)}{\partial y}. \qquad \textbf{[S18]}$$

Expression Eq. S18 can be solved for the costate for crayfish:

$$\lambda_x(x,y) = \left[\left[\rho - \frac{\partial G(x,y)}{\partial y}\right]\left[p - \frac{w_y}{y}\right] - \frac{w_y}{y^2}G(x,y)\right] \Big/ \left[\partial F(x,y)/\partial y\right]. \qquad \textbf{[S19]}$$

Take the time derivative of Eq. S19,

$$\frac{d\lambda_x(x,y)}{dt} = \frac{\partial \lambda_x(x,y)}{\partial x}[F(x,y) - h_x] + \frac{\partial \lambda_x(x,y)}{\partial y}[G(x,y) - h_y], \qquad \textbf{[S20]}$$

where the partial derivatives in Eq. S20 are derived from Eq. S19. Eqs. S16, S19, and S20 can be substituted into the adjoint condition Eq. S12 for crayfish:

$$\begin{aligned} &\frac{\partial \lambda_x(x,y)}{\partial x}[F(x,y) - h_x] + \frac{\partial \lambda_x(x,y)}{\partial y}[G(x,y) - h_y] \\ &\quad = \rho\lambda_x(x,y) - \left[p - \frac{w_y}{y}\right]\frac{\partial G(x,y)}{\partial x} \\ &\qquad - \lambda_x(x,y)\frac{\partial F(x,y)}{\partial x} - \frac{w_x}{x^2}h_x. \end{aligned} \qquad \textbf{[S21]}$$

Eq. S21 can be solved for the following singular feedback rule, which is valid only when σ_y vanishes (otherwise, Eq. S15 indicates h_y equals either zero or $h_y^{\max}$):

$$h_y^*(x,y)|_{h_x} = G(x,y) + \frac{\dfrac{\partial \lambda_x(x,y)}{\partial x}[F(x,y) - h_x] + \left[\dfrac{\partial F(x,y)}{\partial x} - \rho\right]\lambda_x(x,y) + \left[p - \dfrac{w_y}{y}\right]\dfrac{\partial G(x,y)}{\partial x} + \dfrac{w_x}{x^2}h_x}{\partial \lambda_x(x,y)/\partial y}. \qquad \textbf{[S22]}$$

The feedback rule Eq. S22 is conditional on h_x. A singular solution for bass, for a particular nonsingular value of h_x, is called a partial singular solution for bass conditional on h_x. A double singular solution, arising when h_x is also singular, is explored in scenario IV below.

Consider the special case in which $h_x = 0$. The system dynamics are derived by substituting $h_y(x, y)$ and $h_x = 0$ into Eqs. S1 and S2. However, given the initial states of the world, x_0 and y_0, we must determine whether the optimal solution involves $h_y(x, y) = 0$, $h_y(x, y) = h_y^{\max}$, or $h_y(x, y) = h_y^*(x,y)|_{h_x=0}$. We proceed by considering each solution type in turn (following the approach of Mesterton-Gibbons) (5), as illustrated in Fig. S1, *i–iii*, where black arrows are potential trajectories for the particular solution being considered. The dotted-dashed curve in Fig. S1, *i–iii* represents the $dx/dt = 0$ isocline, which is the same in each part (because $h_x = 0$ in each case). The dashed curve in Fig. S1, *i–iii* represents the $dy/dt = 0$ isocline for the particular choice of $h_y(x, y)$. In Fig. S1, *ii*, with $h_y(x, y) = h_y^{\max}$, the $dy/dt = 0$ isocline lies outside the positive orthant.

Trajectories and isoclines for Fig. S1 (and also Figs. S2 and S3) are determined numerically using Mathematica 7.0 (6) and the model specification and parameters from *SI Text S1*. The stability properties of the interior equilibria in Fig. S1, *i* and *ii* are determined by calculating the eigenvalues of the Jacobian matrix for the system, evaluated at each equilibrium. Each (locally) stable equilibrium has two negative eigenvalues. Each conditionally stable (saddle) equilibrium has one positive and one negative eigenvalue. The unstable focus equilibrium in Fig. S1, *iii* has imaginary eigenvalues with positive real parts. Separatrices are derived following Conrad and Clark (7).

Setting $h_y(x, y) = 0$ $\forall t$. The first possibility is to set $h_y(x, y) = 0$ $\forall t$, so that neither species is harvested (Fig. S1, *i*). Two equilibria are locally stable (A^0 and B^0) and one is conditionally stable

(saddle), C^0, so the system always moves to either A^0 or B^0 (unless the system happens to start on a separatrix, which occurs with zero probability). The strategy of $h_y = h_x = 0\ \forall t$ is not optimal for our parameterization. This strategy yields SW = 0, regardless of the initial conditions. However, the system eventually moves to equilibrium A^0 or B^0, with $p > w_y/y$ at either of those points (which is verified numerically). Then setting $h_y > 0$ for even an instant yields SW > 0. Hence, there are incentives to move away from A^0 or B^0, and so neither can be a long-run optimum. This means $h_y(x, y) = 0$ can be only a short-term component of an optimal trajectory.

Setting $h_y(x, y) = h_y^{max}$ $\forall t$. Consider setting $h_y(x, y) = h_y^{\max}\ \forall t$ (Fig. S1, *ii*). Extinction of y is the global equilibrium in this case. This strategy cannot be a long-run optimum. To see this, note $\lambda_y < p - w_y/y$ is necessary for $h_y(x, y) = h_y^{\max}$ to be optimal (from Eq. **S15**). This necessary condition implies $\lambda_y \to -\infty$ as $y \to 0$. However, because bass contribute only positively to SW, λ_y must be nonnegative in an optimal solution (8). Hence, $h_y(x, y) = h_y^{\max}$ can be only a short-term component of an optimal trajectory.

Partial singular solution for $h_y(x, y)$. Finally, the case of $h_y(x,y) = h_y^*(x,y)|_{h_x=0}$ (Fig. S1, *iii*) yields two conditionally stable equilibria (A^y and B^y) and one unstable focus equilibrium, C^y. The separatrices leading to A^y and B^y are illustrated by the bold trajectories a^y and b^y. Other trajectories are also illustrated. The light gray trajectories correspond to $h_y^*(x,y)|_{h_x=0} < 0$ and thus are infeasible. Below the separatrices, trajectories lead to bass extinction, which we have already argued does not satisfy the optimality conditions. Trajectories above the separatrices lead to the infeasible region, which also cannot be optimal [also, setting $h_y(x, y) = 0$ within the infeasible region is not optimal, as indicated above in relation to Fig. S1, *i*]. Hence, the separatrices are the only trajectories satisfying the necessary conditions for the partial singular solution when $h_x = 0\ \forall t$. The separatrices a^y and b^y therefore represent the switching curve for this case, denoted $\sigma_y|_{h_x=0,\forall t} = 0$.

Optimal solution. Fig. S1, *iv* is a feedback control diagram that "splices" together the solutions that apply in different regions of the state space. The switching curves and the equilibria A^y and B^y come from the singular solution of Fig. S1, *iii*. Along the switching curves, $\sigma_y|_{h_x=0,\forall t} = 0$. Above the switching curves, y is increased and so $\sigma_y|_{h_x=0,\forall t} = p - w_y/y - \lambda_y > 0$ and $h_y(x,y) = h_y^{\max}$ is optimal, as indicated by the trajectories in Fig. S1, *iv* (which are identical to those in Fig. S1, *ii*). Below the switching curves, y is decreased and so $\sigma_y|_{h_x=0,\forall t} = p - w_y/y - \lambda_y < 0$ and $h_y(x,y) = 0$ is optimal, as indicated by the trajectories in Fig. S1, *iv* (which are identical to those in Fig. S1, *i*). This solution means that, for initial points off the switching curve, an optimal strategy is to move to the partial singular solution as quickly as possible along a most rapid approach path (MRAP).

Which separatrix is optimally pursued depends on the initial conditions, as numerical analysis (i.e., comparing the values of SW from starting on and following each saddle path versus moving off the saddle path to pursue to the other) indicates that equilibria A^y and B^y are both locally optimal. We can derive a threshold, which we refer to as the Skiba threshold, dividing the state space into two basins of attraction for optimal management (solving for Skiba points or thresholds generally requires numerical methods) (9). Management is optimally undertaken to move the system as quickly as possible to path a^y when the system is initially to the left of the threshold or to path b^y when the system is initially to the right of the threshold.

The Skiba threshold is an endogenous bioeconomic threshold that reflects both human and ecological interactions given the current institutional arrangements and economic environment. Starting below the separatrices, the Skiba threshold is the do-nothing path that is tangent to path b and then becomes vertical at this tangency. The shape and location of the Skiba threshold differ from those of the decoupled system.

Scenario IV: Management of Both Bass and Crayfish. Suppose the agency can choose harvests for both species (i.e., $\Omega = \{h_x, h_y\}$). The necessary conditions for bass harvests have already been given by Eq. **S15**, with the singular solution for bass defined in Eq. **S22**. We therefore focus on the crayfish sector.

The marginal effects of crayfish harvests on the Hamiltonian are given by

$$\partial H/\partial h_x = \sigma_x = -w_x/x - \lambda_x, \qquad \textbf{[S23]}$$

where σ_x is the switching function for h_x. If $\sigma_x < 0$, no harvests of crayfish should take place ($h_x = 0$) as the marginal value of the harvest is negative. If $\sigma_x > 0$, then harvests are beneficial and h_x should be set as large as possible. A singular path for h_x is followed when $\sigma_x = 0$. The optimal level of h_x follows a feedback rule, denoted $h_x(x, y)$, defined by

$$h_x(x,y) = \begin{cases} h_x^{\max} & iff\ \ \sigma_x > 0 \\ h_x^*(x,y) & iff\ \ \sigma_x = 0 \\ 0 & iff\ \ \sigma_x < 0, \end{cases} \qquad \textbf{[S24]}$$

where the superscript * denotes the state variables are evaluated along a singular path.

Consider the singular solution for crayfish harvests, in which case σ_y vanishes:

$$\lambda_x = -w_x/x. \qquad \textbf{[S25]}$$

Taking the time derivative of Eq. **S25** yields

$$\dot{\lambda}_x = \frac{w_x}{x^2}\,\dot{x} = \frac{w_x}{x^2}\,[F(x,y) - h_x]. \qquad \textbf{[S26]}$$

Substituting conditions Eqs. **S25** and **S26** into the adjoint condition Eq. **S12** for crayfish yields

$$\frac{w_x}{x^2}[F(x,y) - h_x] = \rho\left[-\frac{w_x}{x}\right] - \frac{w_x h_x}{x^2} - \lambda_y \frac{\partial G(x,y)}{\partial x} + \frac{w_x}{x}\,\frac{\partial F(x,y)}{\partial x}. \qquad \textbf{[S27]}$$

Expression Eq. **S27** can be solved for the costate for bass:

$$\lambda_y(x,y) = \left[\left[\rho - \frac{\partial F(x,y)}{\partial x}\right]\left[-\frac{w_x}{x}\right] - \frac{w_x}{x^2}\,F(x,y)\right] \Big/ \left[\partial G(x,y)/\partial x\right]. \qquad \textbf{[S28]}$$

Take the time derivative of Eq. **S28**,

$$\frac{d\lambda_y(x,y)}{dt} = \frac{\partial \lambda_y(x,y)}{\partial x}[F(x,y) - h_x] + \frac{\partial \lambda_y(x,y)}{\partial y}[G(x,y) - h_y], \qquad \textbf{[S29]}$$

where the partial derivatives in Eq. **S29** are derived from Eq. **S28**. Eqs. **S25**, **S28**, and **S29** can be substituted into the adjoint condition Eq. **S12** for bass:

$$\frac{\partial \lambda_y(x,y)}{\partial x}\,[F(x,y) - h_x] + \frac{\partial \lambda_y(x,y)}{\partial y}\,[G(x,y) - h_y]$$

$$= \left[\rho - \frac{\partial G(x,y)}{\partial y}\right]\lambda_y(x,y) - \frac{w_y}{y^2}\,h_y + \frac{w_x}{x}\,\frac{\partial F(x,y)}{\partial y}. \qquad \textbf{[S30]}$$

Eq. **S30** can be solved for the following singular feedback rule, which is valid only when the switching function σ_x vanishes (otherwise, Eq. **S24** indicates h_x equals either zero or $h_x^{\max}$):

$$h_x^*(x,y)|_{h_y} = F(x,y) + \frac{\frac{\partial \lambda_y(x,y)}{\partial y}\left[G(x,y) - h_y\right] + \left[\frac{\partial G(x,y)}{\partial y} - \rho\right]\lambda_y(x,y) - \frac{w_x}{x}\frac{\partial F(x,y)}{\partial y} + \frac{w_y}{y^2}h_y}{\partial \lambda_y(x,y)/\partial x}. \quad \text{[S31]}$$

As with Eq. S22, the feedback rule Eq. S31 is conditional on bass harvests.

Double singular solution. Both switching functions simultaneously vanish in the case of a double singular solution. As indicated in our discussion of scenario III, the switching function associated with one species may be conditional on how the other species is managed.

We begin by deriving the switching function for crayfish harvests, conditional on bass management. Suppose managers choose bass harvests such that $\sigma_y = [p - w_y/y] - \lambda_y = 0$ and the adjoint condition Eq. S12 for bass is satisfied, so that λ_x is defined by Eq. S19. The switching function for crayfish harvests vanishes in this case when Eq. S25 is also satisfied:

$$\left[\left[\rho - \frac{\partial G(x,y)}{\partial y}\right]\left[p - \frac{w_y}{y}\right] - \frac{w_y}{y^2}G(x,y)\right] \Big/ \left[\partial F(x,y)/\partial y\right] = -\frac{w_x}{x}. \quad \text{[S32]}$$

Eq. S32 is depicted in Fig. S2 as curve $\sigma_x|_{\sigma_y=0} = 0$. This notation indicates Eq. S32 defines the switching function for crayfish, conditional on $\sigma_y = 0$.

As $\sigma_x|_{\sigma_y=0} = 0$ does not require adjoint condition Eq. S12 for crayfish to be satisfied, this switching curve does not require a partial singular solution for bass (as both adjoint conditions are necessary in that case). However, any partial singular arc for bass that intersects switching curve $\sigma_x|_{\sigma_y=0} = 0$ must yield a double singular solution at the point of intersection. Also, the switching curve $\sigma_x|_{\sigma_y=0} = 0$ helps determine the optimal value of h_x when $h_y = h_y^*$. To the left of the downward-sloping portion of $\sigma_x|_{\sigma_y=0} = 0$, x is sufficiently small that $\lambda_x(x, y) > -w_x/x$ and $h_x = 0$ is optimal when $h_y = h_y^*$. The same is true below $\sigma_x|_{\sigma_y=0} = 0$, as this represents a single iso-sector. The opposite is true to the right of and above $\sigma_x|_{\sigma_y=0} = 0$: $\lambda_x(x, y) < -w_x/x$ and $h_x = h_x^{\max}$ is optimal when $h_y = h_y^*$. This result means scenario III's equilibrium A^y, which lies to the right of $\sigma_x|_{\sigma_y=0} = 0$ (Fig. S2) and involves $h_x = 0$ and $h_y = h_y^*$, cannot be a long-run optimum for scenario IV.

We now derive the switching function for bass harvests, conditional on crayfish management. Suppose managers choose crayfish harvests such that $\sigma_x = -w_x/x - \lambda_x = 0$ and the adjoint condition Eq. S12 for crayfish is satisfied, so that λ_y is defined by Eq. S28. The switching function for bass harvests vanishes in this case when Eq. S16 is also satisfied:

$$\frac{\left[\rho - \frac{\partial F(x,y)}{\partial x}\right]\left[-\frac{w_x}{x}\right] - \frac{w_x}{x^2}F(x,y)}{\partial G(x,y)/\partial x} = p - \frac{w_y}{y}. \quad \text{[S33]}$$

Eq. S33 is depicted in Fig. S2 as curve $\sigma_y|_{\sigma_x=0} = 0$, and the interpretation is analogous to that of curve $\sigma_x|_{\sigma_y=0} = 0$. Specifically, Eq. S33 is based on the assumptions that both switching functions vanish and that adjoint condition Eq. S12 for crayfish is satisfied. If a partial singular arc for crayfish passes through the curve $\sigma_y|_{\sigma_x=0} = 0$, then it becomes optimal for h_y to take on its singular value at the point of intersection, resulting in a double singular solution at that point. Below $\sigma_y|_{\sigma_x} = 0$, we have $\lambda_y(x,y) > p - w_y/y$ and $h_y = 0$ is optimal when $h_x = h_x^*$. Above $\sigma_y|_{\sigma_x=0} = 0$, we have $\lambda_y(x,y) < p - w_y/y$ and $h_y = h_y^{\max}$ is optimal when $h_x = h_x^*$.

Conditions Eqs. S32 and S33 must both hold at a double singular solution. As these conditions are two variables in two unknowns (x and y), there can generally be only a discrete number of pairs of double singular values for x and y. Two potential solutions emerge in Fig. S2, at points A^* and B^*. These points are steady states conditional on a double-singular control rule. Using Eq. S16 for $\lambda_y(x, y)$, so that $\partial\lambda_y(x, y)/\partial y = w_y/y^2$, Eq. S32 implies the numerator in the second right-hand side (RHS) term in Eq. S31 vanishes, resulting in $h_x^*(x,y) = F(x,y)$ and hence $\dot{x} = 0$. Analogously, using Eq. S25 for $\lambda_x(x, y)$, so that $\partial\lambda_x(x, y)/\partial x = w_x/x^2$, Eq. S33 implies the numerator in the second RHS term in Eq. S25 vanishes, resulting in $h_y^*(x,y) = G(x,y)$ and hence $\dot{y} = 0$.

The double singular equilibrium B^* is ruled out as an optimality candidate because, although it satisfies the standard necessary conditions shown above, it does not satisfy Kelley's condition, an additional necessary condition for the optimality of singular arcs (10). In our model, Kelley's condition is the $k = 1$ case of the generalized Legendre–Clebsch condition, $(-1)^k\partial[(d/dt)^{2k}H_{\mathbf{u}}]/\partial\mathbf{u} \leq 0$, where $\mathbf{u}$ is the control vector (11). This is a second-order condition for local optimality.

The double singular point A^* satisfies Kelley's condition and is therefore a candidate long-run optimum. However, what is the optimal approach path(s) to A^*? An optimal approach path, from a particular starting value, must involve partially singular and/or nonsingular choices for the controls because it is not possible to approach A^* on a double singular arc.

In the following subsections, we analyze optimal approach paths to A^* and also the possibility of alternative optimality candidates. First, however, we use Fig. S2 to rule out all but two categories of possible candidate paths and equilibria involving partial singular arcs. Consider scenarios where it is optimal, for some interval of time, to follow an arc that is singular for h_j ($j = x$ or y) but not h_i ($j \neq i$). Denote this partially singular arc by $\sigma_j|_{h_i \neq h_i^*} = 0$. Following a partially singular arc $\sigma_j|_{h_i \neq h_i^*} = 0$ for some time interval *may* be optimal along an approach trajectory to A^*, and it *will* be optimal for attaining alternative long-run optimality candidates. [We have already indicated the no-harvest equilibria from Fig. S1 are not optimal, and continued application of maximum harvest rates for one or both controls will result in extinction of one or more species—which cannot be optimal given our specification of costs and benefits (4). Therefore, an optimal interior equilibrium other than A^* can arise only when at least one control is singular and the other is zero.] The only optimality candidates for such scenarios will be those arcs that intersect A^* or that attain an equilibrium before crossing a switching curve $\sigma_i|_{\sigma_j=0} = 0$ ($i \neq j$).

For instance, the partially singular arc a^y (also denoted $\sigma_y|_{h_x=0} = 0$) in Fig. S2 neither intersects A^* nor attains an equilibrium prior to crossing the switching curve $\sigma_x|_{\sigma_y=0} = 0$. Rather, arc a^y crosses $\sigma_x|_{\sigma_y=0} = 0$ at the point $\widehat{C} \neq A^*$. If it is optimal to proceed along arc a_y, then there is no incentive to leave arc a^y before reaching $\widehat{C}$, as $\partial H/\partial h_y = 0$ is maintained along this arc. Hence, the system eventually reaches $\widehat{C}$, which should also be optimal if arc a^y is optimal. Once at $\widehat{C}$, both switching functions vanish so that a double singular solution should result. However, as described above, the adjoint condition for crayfish is not satisfied at $\widehat{C}$, implying this point and hence arc a^y cannot be optimal (at least when h_x is chosen optimally; path a^y was previously deemed optimal for the case in which h_x was exogenously restricted to be zero). More generally, any partial singular arc for bass that crosses $\sigma_x|_{\sigma_y=0} = 0$ anywhere other than the double singular point A^* cannot be optimal. The same is true for partial

singular arcs for crayfish that cross $\sigma_y|_{\sigma_x=0} = 0$ anywhere other than A^*.

Therefore, candidate paths to A^* must involve a partial singular arc that leads directly to A^* or else the use of nonsingular controls to move directly from the initial states to A^*. Following a partial singular arc, such as the portion of arc b^y to the right of $\sigma_x|_{\sigma_y=0}$ (Fig. S2), to an equilibrium such as B^y may be locally optimal if the path does not involve crossing another switching curve. However, we are able to rule out such candidate paths below.

Partial singular solution for bass harvests when $h_x = 0$. In scenario III we analyzed optimal management of bass when crayfish harvests *never* occurred (i.e., h_x was exogenously 0 $\forall t$). In that scenario, trajectories a^y and b^y (Fig. S1, *iv*) were chosen to attain A^y and B^y, respectively, because these points were the only possible long-run equilibria. Now consider whether $h_x = 0$ may hold temporarily along a singular arc leading to the double singular point A^*. A unique partial singular arc of this type, a^* in Fig. S3, *i*, lies to the left of $\sigma_x|_{\sigma_y=0} = 0$, ensuring $h_x = 0$ satisfies the necessary conditions along this path. Trajectory a^* is the optimal switching curve for bass harvests conditional on $h_x = 0$. Denote this switching curve by $\sigma_y^*|_{h_x=0} = 0$, where the superscript * indicates this trajectory intersects A^*. Once A^* is attained, h_x optimally switches from 0 to its singular value.

Partial singular solution for crayfish harvests when $h_y = 0$. A phase plane for the case of a partial singular solution for crayfish harvests (Eq. **S31**), conditional on $h_y = 0$, is presented in Fig. S3, *ii*. Light gray trajectories involve infeasible values of h_x and therefore cannot contribute to an optimal solution. In particular, the gray curve Z is an asymptote, with $h_x^*|_{h_y=0} \to \infty$ on the black trajectories close to Z, whereas $h_x^*|_{h_y=0} \to -\infty$ on the gray trajectories close to Z.

Point A^x represents the only feasible partial singular equilibrium, although it is easily ruled out as an optimality candidate. This result is because only costs (no benefits) are generated at this equilibrium, and also along trajectories to it, as removing crayfish produces no benefits in this model if the bass fishery remains closed.

The next question is whether a partially singular crayfish trajectory exists that can move the system to point A^*. Trajectory b^* accomplishes this task and therefore represents the singular arc or switching curve for crayfish harvests conditional on $h_y = 0$. Note that trajectory b^* is interrupted by Z, although we treat it as a continuous trajectory. This is because $h_x^*|_{h_y=0} \to \infty$ as b^* approaches Z from the right and also as b^* leaves Z from the left. An impulse control is therefore optimally applied to bridge the gap. We denote this switching curve by $\sigma_x^*|_{h_y=0} = 0$.

Having identified path b^*, we can now show that this path yields larger economic surplus than path b^y, so that path b^* is locally optimal whereas path b^y is not. Suppose the system were currently at point B^y, which is the terminus of path b^y and lies slightly above path b^* (although this is difficult to see in Fig. S3, *ii*). If this point were locally optimal, then SW would be maximized by staying put. However, SW is increased by moving to path b^* if b^* is optimal relative to B^y. The optimized Hamiltonian is a welfare measure proportional to SW that can be used to compare alternative strategies (12).

The optimized Hamiltonian associated with path b^y, denoted H^y, involves $\lambda_y = p - w_y/y$ and $h_x = 0$. Evaluating H^y at $B^y = (x^y, y^y)$, where $F(x^y, y^y) = 0$, yields

$$H^y = (p - w_y/y^y)G(x^y, y^y). \quad \textbf{[S34]}$$

Now consider an alternative strategy of moving from B^y to b^*. Starting at point B^y, suppose we set $h_y = h_y^{\max}$ (while retaining $h_x = 0$) to initiate a downward movement from point B^y to path b^*. The decision to set $h_y = h_y^{\max}$ results in an alternative value of λ_y, denoted λ_y^{alt}, such that $\lambda_y^{\text{alt}} < p - w_y/y$. The Hamiltonian associated with this choice, denoted H^{alt}, evaluated at point B^y, is

$$H^{\text{alt}} = [(p - w_y/y^y) - \lambda_y^{\text{alt}}]h_y^{\max} + \lambda_y^{\text{alt}}G(x^y, y^y) \quad \textbf{[S35]}$$

The difference between Eqs. **S34** and **S35** is

$$H^y - H^{\text{alt}} = \left[\left(p - w_y/y^y\right) - \lambda_y^{\text{alt}}\right]\left[G(x^y, y^y) - h_y^{\max}\right] < 0. \quad \textbf{[S36]}$$

Hence it is optimal to move to the alternative path. Our approach of using a discrete change in h_y to compare two strategies is analogous to Rondeau's (12) approach of using a marginal change in his control to compare two strategies. Our result in Eq. **S36** is also analogous to Rondeau's result that the change in the Hamiltonian equals the change in the costate times the change in the corresponding stock. Note that the movement from B^y to the alternative path is not necessarily optimal (as we indicate below, a leftward jump from point B^y to path b^* would be truly optimal). However, as this movement improves SW, B^y cannot be a local optimum.

Optimal solution. Fig. S3, *iii* depicts the optimal feedback control diagram (not phase plane) derived after considering all combinations of singular and nonsingular controls, assuming for simplicity that impulse controls are possible (i.e., $h_j^{\max} \to \infty$). [We have assumed impulse controls for this case because this assumption simplifies the derivation of the curves $\tilde{h}_x$ and $\tilde{h}_y$, defined below, along with the welfare comparison below in Eq. **S39**. The qualitative results would not be affected, however, by assuming the controls are bounded from above. In that case, adjustment to a singular path may be more sluggish, resulting in the curves $\tilde{h}_x$ and $\tilde{h}_y$ being positively sloped. We also note that, although our earlier analysis of the partial singular solutions was based on the assumption that the controls are bounded from above, those results would still hold even in the absence of these bounds (so that an impulse control for h_j is optimal whenever $\partial H/\partial h_j > 0$). A feedback control diagram splices together the various types of solutions that we have examined (i.e., fully constrained, partial singular, and double singular) (13). The optimal controls are specified in the form $\{h_x, h_y\}$ as feedback rules that depend on the current values of x and y, as indicated in the various regions of the diagrams.

Fig. S3, *iii* indicates A^* is a unique long-run optimum. The optimal controls for various regions of the state space are governed by the two switching curves defined above and the curves $\tilde{h}_x$ and $\tilde{h}_y$. Although they also divide the state space into different control regions, $\tilde{h}_x$ and $\tilde{h}_y$ are not switching curves. Clark et al. (13) also found it optimal to change controls at points not lying on a switching curve [see the vertical arrow below the end of their switch curve σ_2, at the point (x^*, K^*), in their figures 1–4]. We can show that such changes in controls are optimal.

Consider the curve $\tilde{h}_x$, which is the vertical segment intersecting A^* from above. Suppose the system is initially at a point on $\tilde{h}_x$, which we denote as (x^*, $\hat{y}$), with $\hat{y} > y^*$. As $\tilde{h}_x$ is not a switching curve (verified numerically), an optimal harvest strategy at this initial point must involve the application of nonsingular controls to move to A^* or to one of the partial singular trajectories. Clearly, combinations involving $h_y = 0$ will fail to accomplish this goal, and so $h^y = h_y^{\max}$ is optimal (which makes economic sense as well: relative to the optimum at A^*, the larger value of y implies $p - w_y/y$ is increased relative to λ_y). If we set $h_x = 0$ while applying h_y as an impulse control, the system moves directly to A^* and SW is

$$\begin{aligned} \text{SW}^* &= p(\hat{y} - y^*) - w_y \ln(\hat{y}/y^*) \\ &\quad + \left[(p - w_y/y^*)G(x^*, y^*) - w_x F(x^*, y^*)/x^*\right]/\rho. \end{aligned} \quad \textbf{[S37]}$$

Alternatively, if we apply both harvests as impulse controls, then we would move southwest to a point on a^*. Define this point by

$A' = (x', y')$, with $x' < x^*$ and $y' < y^*$. Then the SW associated with these impulse controls is

$$SW' = p(\hat{y} - y') - w_y \ln(\hat{y}/y') - w_x \ln(x^*/x') + \int_0^\infty \left[(p - w_y/y)h_y - w_x h_x/x\right] e^{-\rho t} dt;\ x_0 = x', y_0 = y'. \quad \text{[S38]}$$

The difference in net benefits between these two strategies is

$$SW' - SW^* = p(y^* - y') - w_y ln(y^*/y') - w_x \ln(x^*/x') + \int_0^\infty \left[(p - w_y/y)h_y - w_x h_x/x\right] e^{-\rho t} dt - \left[(p - w_y/y^*)G(x^*, y^*) - w_x F(x^*, y^*)/x^*\right]/\rho$$

$$x_0 = x',\ \ y_0 = y'. \quad \text{[S39]}$$

This difference equals the net benefits of using impulse controls to move from A^* to A', which is negative if A^* is the long-run optimum. Thus, it is optimal to set $h_x = 0$ and apply h_y as an impulse control, to move along a MRAP to A^*. The same approach can be used to show that, to the right of $\tilde{h}_x$, it is optimal to set $h_x = 0$ and apply h_y as an impulse control to move along a MRAP to a^*.

A similar analysis yields identical results with respect to curve $\tilde{h}_y$. Above $\tilde{h}_y$, it is optimal to apply both controls as impulse controls, to move along a MRAP to A^*. On (below) $\tilde{h}_y$, it is optimal to set $h_y = 0$ and apply h_x as an impulse control, to move along a MRAP to A^* (to b^*).

The feedback rules in Fig. S3, *iv* indicate that the optimal solution, starting from any initial value of x and y, is to move along a MRAP to point A^*, path a^*, or path b^*—whichever can be attained more quickly. From there, A^* is maintained or else path a^* or b^* is followed until A^* is attained. Note that there is no Skiba (bioeconomic) threshold in this case, as the species are managed to attain a unique long-run equilibrium.

Sensitivity Analysis. Table S2 reports the results of a sensitivity analysis designed to examine the robustness of our qualitative results that weak institutions can result in poor outcomes, institutions of intermediate strength can result in multistability, and strong institutions can promote stable, desired outcomes. For each management scenario, we analyzed the model by changing the value of one parameter, while holding the others constant at their benchmark values (Table S1).

First consider the ecological parameters. These parameters were either halved or doubled to reduce the likelihood of multistability in the decoupled model. In particular, the change in α increases the likelihood of outbreak, whereas changes in the other parameters increase the likelihood of non-outbreak. The results are most sensitive to changes in the competition and predation parameters, α, β, and δ. The decrease in α results in a globally stable outbreak equilibrium, whereas the indicated changes in β and δ result in a globally stable non-outbreak equilibrium. Regardless, for all three scenarios, management under weak institutions (SESs I and II) still results in a globally stable outbreak equilibrium, whereas management under strong institutions (SES IV) still results in a non-outbreak equilibrium.

With institutions of intermediate strength (SES III), we find multiple equilibria still arise for the case of 2δ, even though the decoupled model results in a unique (non-outbreak) equilibrium. This result is because the increased predation of bass on crayfish (due to a larger δ) is offset by human harvesting of bass. When β is decreased (crayfish exert less competition on bass), we find an outbreak equilibrium is globally stable under SES III even though the non-outbreak equilibrium is stable in the decoupled model. The reason is that the benefits of leaving more bass in situ, to keep the crayfish population under control, are reduced in this scenario relative to the benchmark case. The result is an outbreak equilibrium, although with more bass and fewer crayfish than in the outbreak equilibrium of the benchmark case. Finally, the reduction in α results in an outbreak equilibrium for both the decoupled model and SES III.

Changes in the economic parameters do not affect the results of the decoupled model, but do affect the SES results. The decrease in p_y has two effects that are offsetting. First, a smaller p_y reduces the incentives to harvest bass, resulting in more bass and a smaller likelihood of an outbreak. Second, a smaller p_y reduces the incentives to prevent an outbreak, as the damages associated with the non-outbreak equilibrium (i.e., loss in bass) are reduced. The overall result is that the number and types of equilibria are unchanged relative to the benchmark case. Finally, the increase in w_x reduces the incentives to harvest crayfish to prevent an outbreak. This outcome has an impact only under SES IV. The non-outbreak equilibrium remains optimal, with slightly more bass arising in this outcome to provide a natural substitute to human predation on crayfish.

1. Drury KLS, Lodge DM (2009) Using mean first passage times to quantify equilibrium resilience in perturbed intraguild predation systems. *Theor Ecol* 2:41–51.
2. Kershner MW, Lodge DM (1995) Effects of littoral habitat and fish predation on the distribution of an exotic crayfish, *Orconectes rusticus*. *J N Am Benthol Soc* 14:414–422.
3. Garvey JE, Stein RA, Thomas HM (1994) Assessing how fish predation and interspecific prey competition influence a crayfish assemblage. *Ecology* 75:532–547.
4. Clark CW (2005) *Mathematical Bioeconomics Optimal Management of Renewable Resources* (Wiley, Hoboken, NJ), 2nd Ed.
5. Mesterton-Gibbons M (1987) On the optimal policy for combined harvesting of independent species. *Nat Resour Model* 2:109–134.
6. Wolfram Research (2009) *Mathematica 7.0* (Wolfram Research, Champaign, IL).
7. Conrad JM, Clark CW (1987) *Natural Resource Economics: Notes and Problems* (Cambridge Univ Press, New York).
8. Leonard D, Van Long N (1998) *Optimal Control Theory and Static Optimization in Economics* (Cambridge Univ Press, Cambridge, UK).
9. Brock WA, Starrett D (2003) Managing systems with non-convex positive feedback. *Environ Resour Econ* 26:575–602.
10. Bryson AE, Jr., Ho YC (1975) *Applied Optimal Control: Optimization, Estimation, and Control* (Hemisphere, New York).
11. Robbins HM (1967) A generalized Legendre-Clebsch condition for the singular cases of optimal control. *IBM J* 11:361–372.
12. Rondeau D (2001) Along the way back from the brink. *J Environ Econ Manage* 42: 156–182.
13. Clark CW, Clarke FH, Munro GR (1979) The optimal exploitation of renewable resource stocks: Problems of irreversible investment. *Econometrica* 47:25–47.

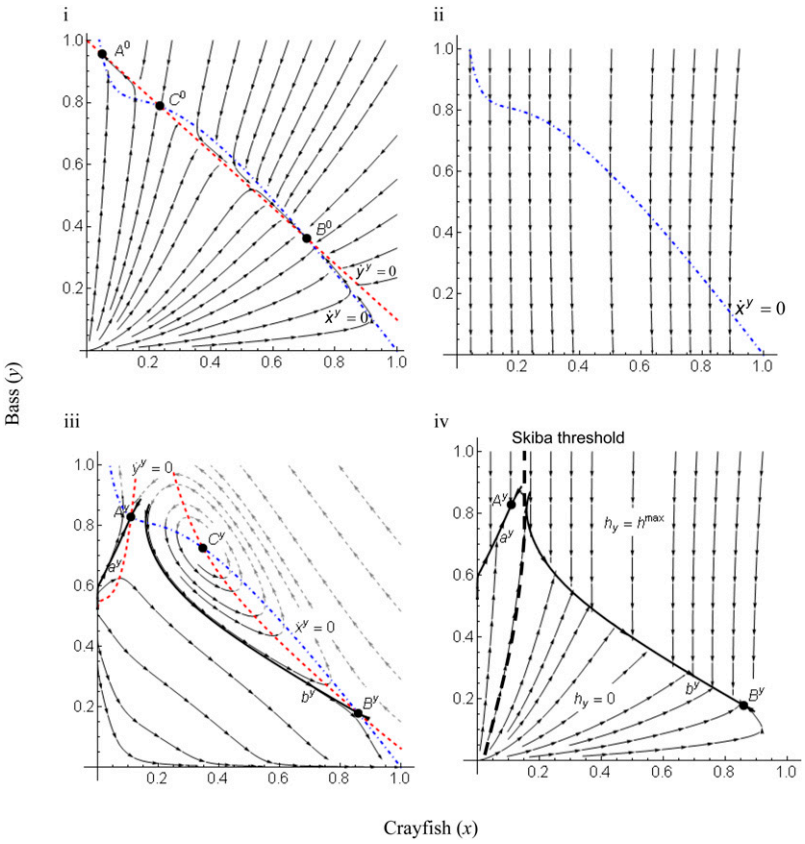

Fig. S1. Deriving the solution for scenario III. (*i*) Phase plane dynamics when $h_y = 0\ \forall t$. The dynamics are the same as those of the decoupled system in Fig. 3 in the main text. (*ii*) Phase plane dynamics when $h_y = h_y^{max}\ \forall t$. All trajectories lead to bass extinction. (*iii*) Phase dynamics when $h_y = h_y^*(x, y)$. Given no crayfish harvests, the $\dot{x}^y = 0$ isocline is the same as in Fig. 3 in the main text. The $\dot{y}^y = 0$ isocline differs from that in Fig. 3 because it reflects feedbacks associated with bass harvests. Equilibrium C^y is an unstable focus, whereas equilibria A^y and B^y are saddle points (conditionally stable). Only trajectory a^y leads to equilibrium A^y, and only trajectory b^y leads to equilibrium B^y. All other trajectories lead to bass extinction or to regions of the state space where singular bass harvests become infeasible (infeasible harvests exist when the singular harvest rule indicates negative harvests; these are illustrated with light gray trajectories). Together, a^y and b^y represent the switching curve for bass harvests, conditional on no crayfish harvests; i.e., $\sigma_y|_{h_x=0,\forall t} = a^y \cup b^y$. (*iv*) Feedback control diagram representing optimal bass harvest levels in different regions of the state space. The dashed "Skiba threshold" divides the state space into two basins of attraction. Along the curves a^y and b^y (including the endpoint equilibria A^y and B^y), bass harvests are applied at their singular values. Above the switching curve, bass harvests are applied at their maximum value. Below the switching curve, bass harvests are zero. Arrows represent sample trajectories. Trajectories for initial points to the left of the threshold move to path a^y and then to equilibrium A^y. Trajectories for initial points to the right of the threshold move to path b^y and then to equilibrium B^y.

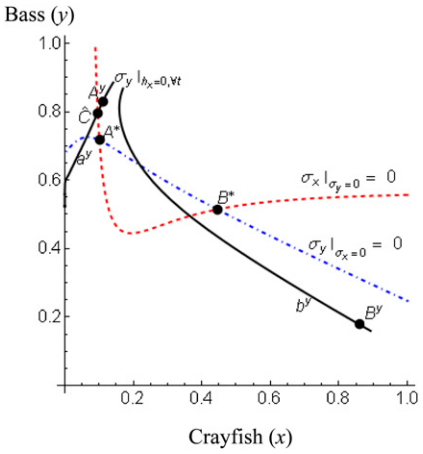

Fig. S2. Switching curves associated with the double singular solution, and a comparison with the partial singular solution for h_y, conditional on $h_x = 0$. The curve $\sigma_x|_{\sigma_y=0}$ is the switching curve for crayfish harvests, conditional on singular bass harvests. The curve $\sigma_y|_{\sigma_x=0}$ is the switching curve for bass harvests, conditional on singular crayfish harvests. The intersection of these curves, at equilibria A^* and B^*, represents the double singular solution. The switching curves and equilibria from Fig. S1, *iii* and *iv*, are superimposed. Point $\hat{C}$ denotes the intersection of path a^y with $\sigma_x|_{\sigma_y=0}$.

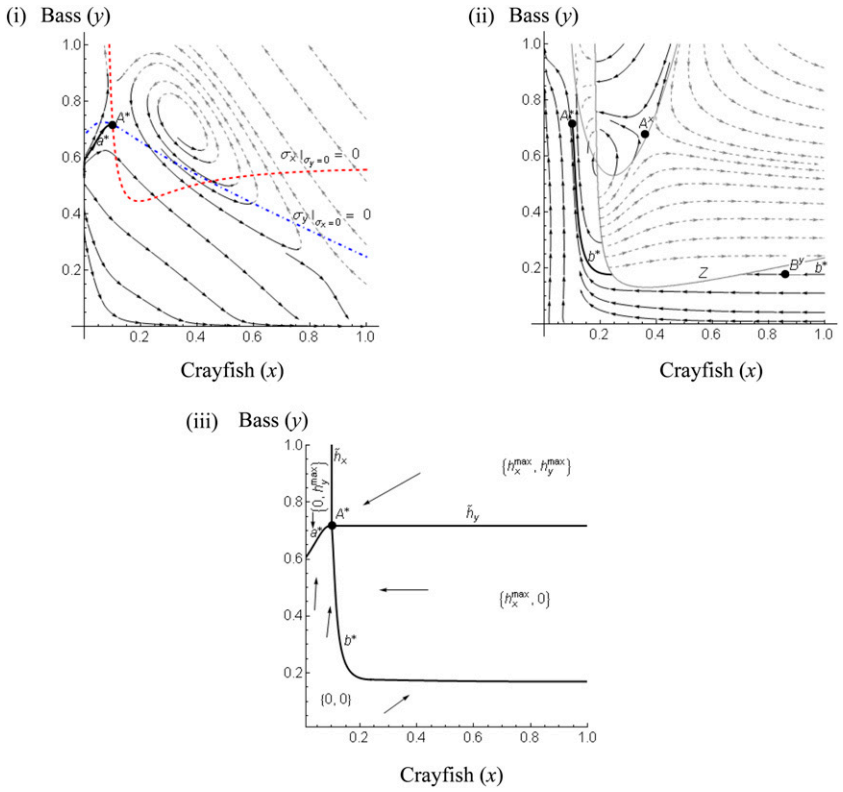

Fig. S3. Deriving the solution for scenario IV. (*i*) Phase dynamics when $h_y = h_y^*(x, y)$ and $h_x = 0$. We show only the trajectories for this case, not the isoclines. Gray trajectories indicate infeasible values of $h_y^*(x, y)$ (when the singular harvest rule indicates negative harvests). The switching curves from Fig. S2 are depicted to indicate the point A^* from Fig. S2. The trajectory a^* is the unique path to A^* for this scenario. (*ii*) Phase plane dynamics when $h_x = h_x^*(x, y)$ and $h_y = 0$. For simplicity, we show only the trajectories for this case, not the isoclines. Gray trajectories indicate infeasible values of $h_x^*(x, y)$. The curve Z represents an asymptote, with $h_x^*|_{h_y=0} \to \infty$ as Z is approached from the right and also as Z is exited from the left. The only equilibrium in this scenario is A^x. Trajectory b^* is the unique trajectory that leads to point A^*, as defined in Fig. S2. (*iii*) Feedback control diagram, reflecting optimal harvesting of both species for different combinations of x and y. There is a globally stable non-outbreak equilibrium, A^*, at which point both harvest levels are set at their singular values. Along the curve a^*, which leads to equilibrium A^*, bass harvests are applied at singular values and crayfish harvests are zero. Along the curve b^*, which leads to equilibrium A^*, crayfish harvests are applied at singular values and bass harvests are zero. In other regions of the graph, crayfish and bass harvests are indicated by the notation $\{h_x, h_y\}$. The curves $\tilde{h}_x$ and $\tilde{h}_y$ divide the state space into regions where different values of the harvest controls are applied. Arrows represent sample trajectories.

Table S1. Parameter values for the simulations

Parameter	Value
α	0.7
δ	0.075
κ	0.1
r	1.5
β	0.9
ε	0.01
K_x	100,000
K_y	1,000
r_x	1.5
P_y	15
w_x	10,000
w_y	1,000
ρ_τ	0.05

Table S2. Sensitivity analysis

Management scenario	Basin type	State variable	Parameter change							
			$(1/2)\alpha$	$(1/2)\kappa$	$(1/2)\beta$	2δ	$2r$	2ε	$(1/2)p_y$	$2w_x$
Decoupled model	Non-outbreak	Crayfish	DNE	−100.0	−10.0	−57.4	0.0	−0.1	0.0	0.0
		Bass	DNE	4.6	2.5	2.6	0.0	0.0	0.0	0.0
	Outbreak	Crayfish	31.3	−0.4	DNE	DNE	0.1	−0.2	0.0	0.0
		Bass	−54.9	0.6	DNE	DNE	−0.3	0.6	0.0	0.0
	Unstable equilibrium	Crayfish	DNE	17.3	DNE	DNE	−0.2	0.4	0.0	0.0
		Bass	DNE	−4.6	DNE	DNE	0.0	0.0	0.0	0.0
SES I, no management; or SES II, crayfish only	Outbreak	Crayfish	2.5	0.0	0.0	−0.6	0.0	0.0	−5.5	0.0
		Bass	0.0	0.0	0.0	0.0	0.0	0.0	100.0	0.0
SES III, bass only	Non-outbreak	Crayfish	DNE	−100.0	DNE	−24.3	−6.1	0.1	−0.4	0.0
		Bass	DNE	−36.8	DNE	−23.1	0.6	0.0	0.0	0.0
	Outbreak	Crayfish	11.0	−0.1	−27.1	−9.9	−1.9	−0.1	−4.2	0.0
		Bass	−39.6	0.3	155.9	41.7	11.7	0.4	25.0	0.0
	Unstable equilibrium	Crayfish	DNE	8.6	DNE	73.0	8.3	0.0	−0.6	0.0
		Bass	DNE	−4.2	DNE	−41.7	−3.0	0.0	0.2	0.0
SES IV, bass and crayfish	Non-outbreak	Crayfish	6.8	−49.8	35.9	−3.0	−29.0	0.1	13.9	13.2
		Bass	−11.3	14.7	1.5	10.6	−14.1	0.0	36.9	32.3

For each management scenario, table entries represent the percentage of change in equilibrium values of the indicated state variable, in response to the indicated parameter change relative to its benchmark value in Table S1 (holding all other parameter values constant). DNE, the indicated equilibrium does not exist.